

15. HIGH-RESOLUTION BIOSTRATIGRAPHY AT THE MIocene/PLIOCENE BOUNDARY IN HOLES 974B AND 975B, WESTERN MEDITERRANEAN¹

Silvia M. Iaccarino,² Maria Bianca Cita,³ Sandra Gaboardi,² and Gian Maria Gruppini²

ABSTRACT

Extended sedimentary sequences encompassing the Miocene/Pliocene boundary were continuously cored in the Tyrrhenian Sea (Hole 974B) and Balearic Basin (Hole 975B) during Ocean Drilling Program Leg 161, and investigated in terms of foraminifer (planktonic and benthic) high-resolution biostratigraphy.

The interval studied includes the earliest part of the Zanclean (Zone MP11) and the Miocene/Pliocene boundary. The lower Zanclean (*Sphaeroidinellopsis* Acme Zone or MP11) is characterized by pelagic sediments in both holes.

Within the lower part of MP11 Zone, cyclically repeated changes in abundance of *Globigerinoides* population have been recognized at both sites and interpreted as caused by astronomical forcing precession cycles. The calibration of these cycles with bioevents like the acme interval of *Sphaeroidinellopsis*, two intervals of *Neogloboquadrina acostaensis* sinistrally coiled, and the first common occurrence (FCO) of *Globorotalia margaritae* led to the identification of five cycles in Hole 974B and six cycles in Hole 975B. Such data indicate that the Hole 975B sequence is more complete than that recorded in Hole 974B, where the first cycle is missing.

The MP11/MP12 boundary, which is based on the FCO of *Globorotalia margaritae* at 5.07 Ma, represents the top of the sequence investigated.

The repopulation of the Mediterranean basin floor by benthic foraminifers is stepwise. The first immigrants were small in size (*Eponides pusillus* and bolivinids) and were found only in Hole 975B. They were followed by *Oridorsalis stellatus*, *Cassidulina subglobosa*, and *Uvigerina peregrina*, which occur at both sites. Such assemblages suggest water masses partially depleted of oxygen at the very base of the Pliocene sequence.

INTRODUCTION

Our knowledge of the high-resolution biostratigraphy at the Miocene/Pliocene boundary is based mainly on land sections of southern Italy (Sicily and Calabria; Langereis and Hilgen, 1991; Sprovieri, 1992, 1993; Di Stefano et al., 1996) and on Site 653 in the Tyrrhenian Sea (Sprovieri, 1993; McKenzie and Sprovieri, 1990). According to the most recent calibration, the Miocene/Pliocene boundary as defined in the Capo Rossello composite section (Hilgen, 1991), falls at 5.33 Ma, five cycles below the Thvera Subchron and two cycles below the base of the *Sphaeroidinellopsis* acme range.

It is well known and documented (Ryan, Hsü, et al., 1973; Hsü et al., 1978; Cita et al., 1978) that the Mediterranean salinity crisis abruptly ended by the influx of Atlantic water, which invaded the different parts of the Mediterranean Basin at the beginning of the Pliocene. This sudden change from continental to marine sediments is clearly recognizable both in land and deep-marine sections where open-marine deposits lie on Lago Mare facies, testifying that this event occurred under subaqueous conditions.

High-resolution stratigraphic studies of this interval revealed a series of paleoceanographic events between the termination of the salinity crisis and the re-establishment of a fully open marine connection with the Atlantic Ocean, which until now were not clearly understood. McKenzie and Sprovieri (1990) recognized three stages, each one indicative of an evolutionary phase of the earliest Mediterranean paleoceanography.

Holes 974B and 975B from Ocean Drilling Program (ODP) Leg 161 were investigated through foraminifer high-resolution biostratig-

raphy to test the completeness of the Pliocene sequence in the two western Mediterranean basins and provide new evidence of the paleoceanographic conditions at the Miocene/Pliocene (M/P) boundary in the central Tyrrhenian Sea (Site 974) and in the South Balearic Basin (Site 975).

Site 978, located in the Eastern Alboran Basin, should have been important to further knowledge of the M/P boundary in the eastern part of the western Mediterranean, but it was not analyzed because the recovery in the boundary interval was very poor (found in only the core-catcher of Core 45R, and there was no recovery of Core 46R). Regardless, the lowermost Pliocene recognized at 161-978A-45R-CC at 630 meters below seafloor (mbsf), belongs to Zone MP11.

MATERIAL AND METHODS

High-resolution sampling encompassing the Miocene/Pliocene boundary was conducted on board the *JOIDES Resolution* at closely spaced intervals of 10 to 20 cm throughout the latest Messinian and lower part of MP11, and 50 to 70 cm through the upper part of MP11 up to the base of MP12. Subsequently, additional samples were taken from Leg 161 cores at the Bremen Repository.

For the shore-based study, the 10-cm³ samples were washed on 63-μm sieves and the residues larger than 125 μm were used for a quantitative study of the planktonic foraminifers. Approximately 300 specimens were counted to achieve a statistically meaningful distribution pattern. The benthic foraminiferal analysis is based on the total number of specimens (fraction >125 μm) and on semiquantitative analysis (<125-μm fraction). Where not specified, the benthic foraminiferal distribution discussed in this chapter is the fraction >125 μm.

The planktonic foraminiferal biostratigraphic scheme proposed for the Mediterranean by Cita (1973, 1975) and amended by Rio et al. (1984) and Sprovieri (1992, 1993) was adopted.

¹Zahn, R., Comas, M.C., Klaus, A. (Eds.), 1999. Proc. ODP, Sci. Results, 161: College Station, TX (Ocean Drilling Program).

²Dipartimento di Scienze della Terra, Università di Parma, Italy.
iaccarin@ipruniv.cce.unipr.it

³Dipartimento di Scienze della Terra, Università di Milano, Italy.

BIOSTRATIGRAPHIC RESULTS

Hole 974B

Hole 974B is located in the central Tyrrhenian Sea ($40^{\circ} 21.362'N$, $12^{\circ} 8.516'E$) (Shipboard Scientific Party, 1996a) very close to Site 652 (ODP, Leg 107) at 3454 m depth (Fig. 1). The sedimentary sequence cored (late Messinian to Pleistocene) is 203 m thick. In the in-

terval investigated, extending from 183.06 mbsf (161-974B-20X-6, 66–68 cm) down to 203.7 mbsf (bottom of the hole), 53 samples were analyzed (Table 1). Samples 974B-22X-6, 66–68 cm, to 22X-4, 93–95 cm (2.73 m thick) are referred to the latest Messinian “non-distinctive” Zone (Iaccarino, 1985); Samples 974B-22X-4, 70–72 cm, to 20X-CC belong to MP11 Zone (15 m thick); Sample 974B-20X-6, 66–68 cm, belongs to MP12 Zone on the basis of the first common occurrence (FCO) of *Globorotalia margaritae*. The Miocene/Pliocene

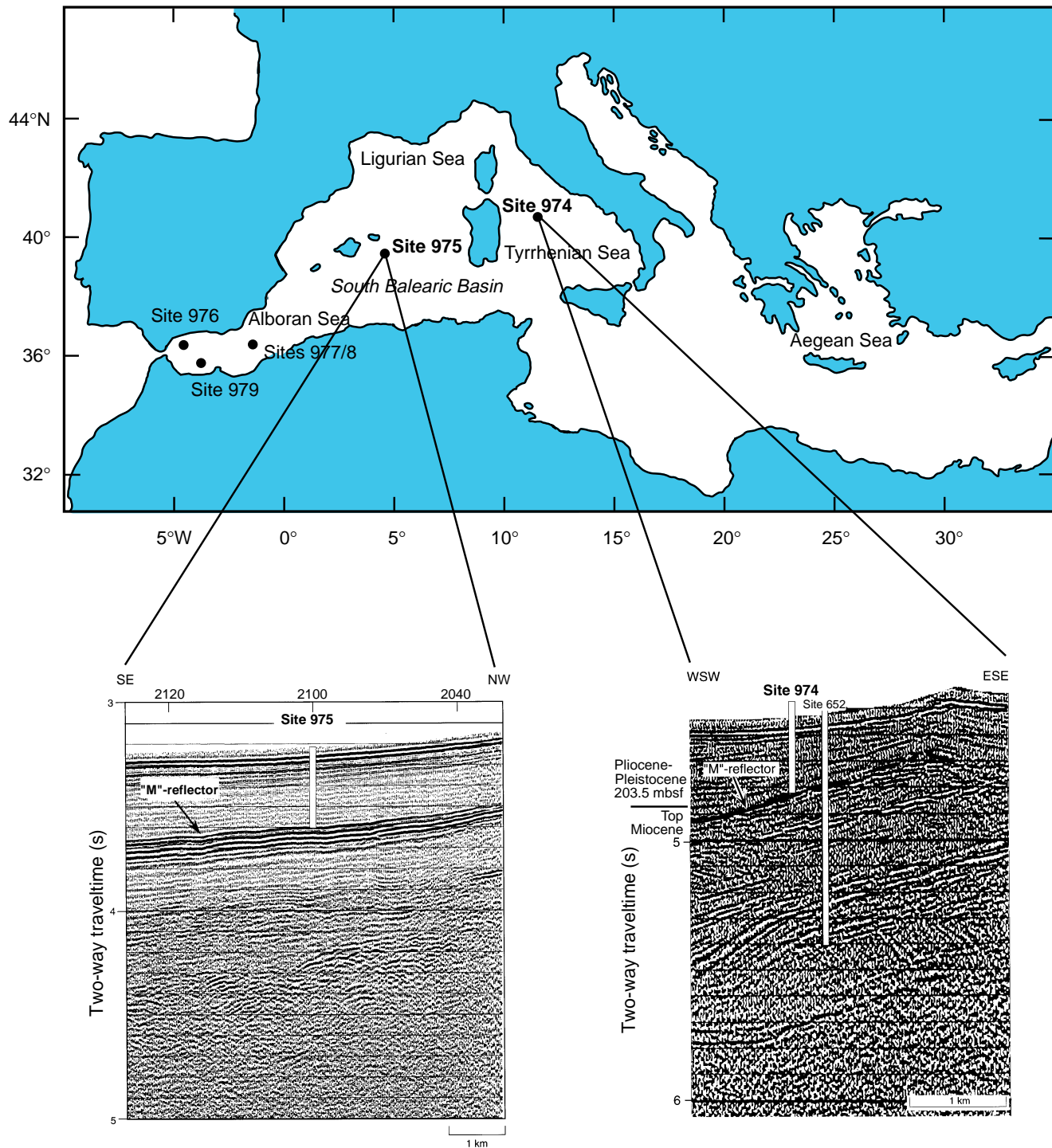


Figure 1. Location map of Sites 974 and 975, and seismic profiles of Site 974 and Site 975.

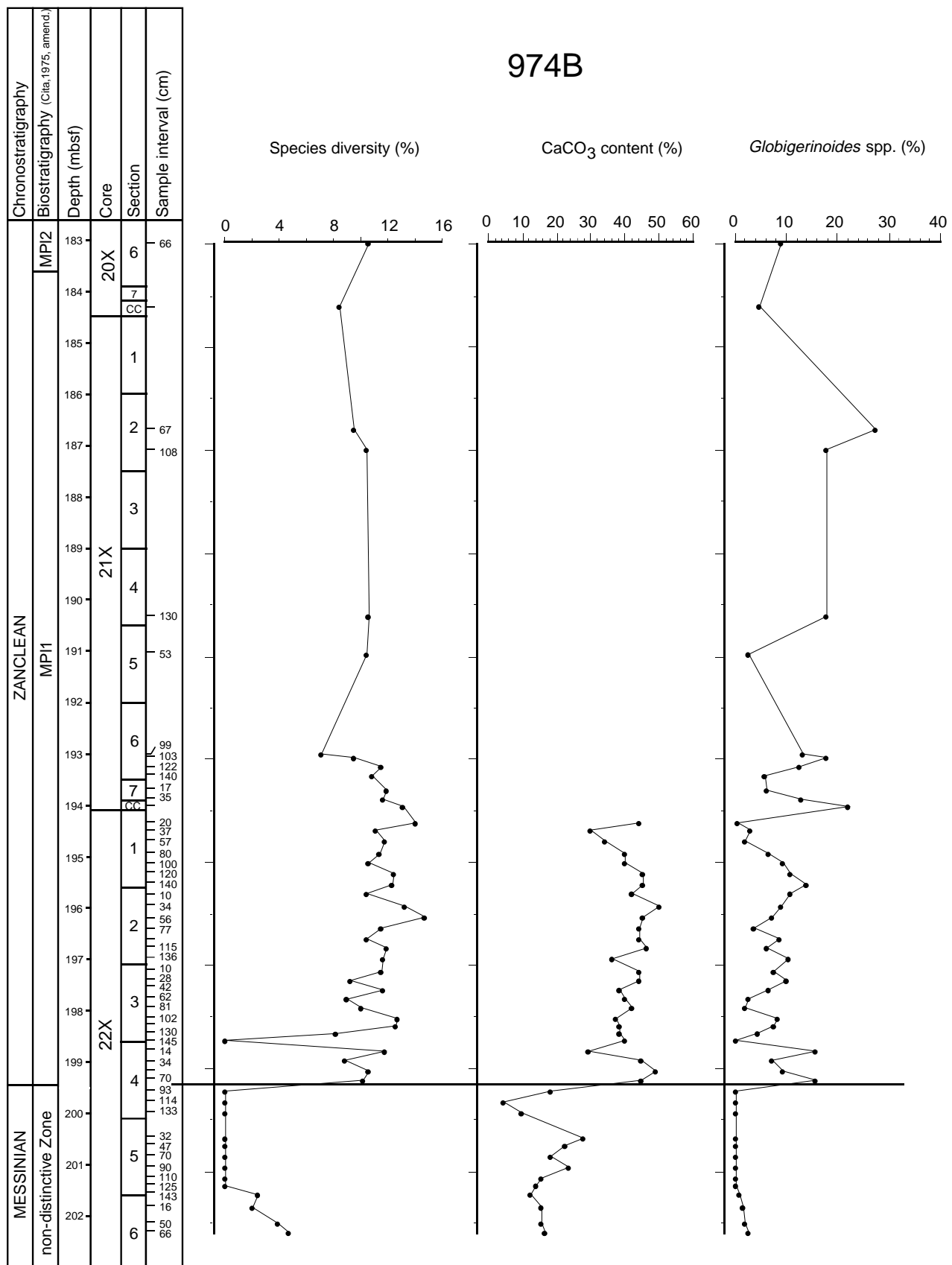


Figure 2. Specific diversity of planktonic foraminifers, CaCO_3 , and *Globigerinoides* spp. curves in Hole 974B.

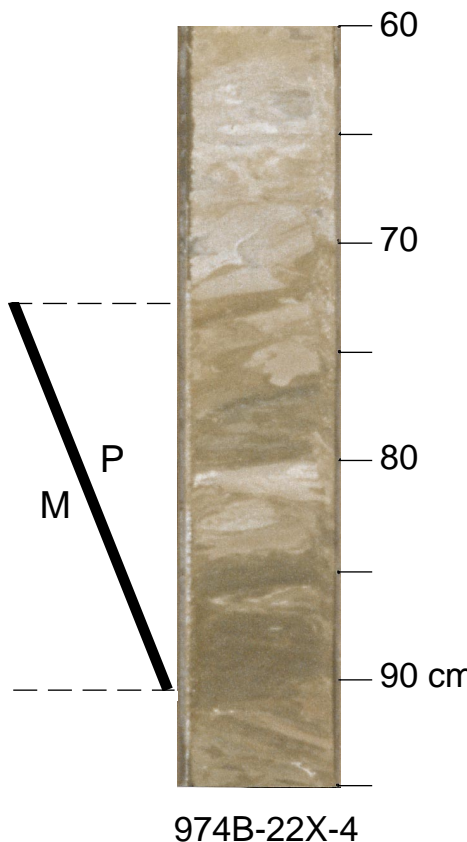


Figure 3. Lithologic variation at the Miocene/Pliocene boundary in Hole 974B. The boundary falls between Samples 161-974B-22X-4, 73 cm, and 22X-4, 91 cm.

Some benthic “events” were recognized:

1. The consistent occurrence of benthic foraminifers from Sample 161-974B-22X-3, 130–132 cm (198.4 mbsf) upward;
2. In the first samples where it is present, the benthic assemblage is dominated by *Oridorsalis* spp. and *Gyroidinoides* spp.;
3. At 197.72 mbsf (Sample 161-974B-22X-3, 62–64 cm) arenaceous foraminifers (represented mainly by *Karreriella bradyi*) first occur;
4. At 195.94 mbsf (Sample 161-974B-22X-2, 34–36 cm) the first increase of the total abundance of benthic foraminifers is recorded. *Oridorsalis stellatus*, *Gyroidinoides laevigatus*, and *Karreriella bradyi* increase and dominate the assemblage;
5. Between 195.94 and 195.70 mbsf (Samples 161-974B-22X-2, 34–36 cm, and 22X-2, 10–12 cm), the increase in abundance of *Globocassidulina subglobosa*, *Nonion* spp., and *Dentalina* spp. first occurs; and
6. From 193.23 mbsf (Sample 161-974B-22X-6, 122–125 cm) upwards, a sharp increase in abundance of benthic foraminifers is observed; only *Dentalina* gr. and *Gyroidinoides* gr. *soldanii* decrease.

Hole 975B

Hole 975B is located on the South Balearic Margin ($38^{\circ}53.786'N$, $4^{\circ}30.596'E$) (Shipboard Scientific Party, 1996b), not too far from Site 372 (Deep Sea Drilling Project, Leg 42) at 2200 m depth (Fig. 1). The entire sedimentary sequence (late Messinian to Pleistocene) is 307 m thick. The investigated interval is 11 m thick, ex-

tending from Sample 161-975B-32X-3, 116–118 cm (at 296.70 mbsf), to Sample 161-975B-33X-CC, 10 cm, below which the evaporites occur. Samples 975B-33X-2, 132–134 cm, to 33X-3, 137–139 cm, belong to the “non-distinctive” Zone of Iaccarino (1985). Samples 975B-32X-4, 40–42 cm, to 33X-2, 130–132 cm, are referred to MP11. Sample 975B-32X-3, 116–118 cm, belongs to MP12.

The quantitative study, carried out on 57 samples, was mostly concentrated on the interval between Sample 161-975B-33X-3, 137–139 cm, and Sample 32X-6, 116–118 cm (Table 3). The Miocene/Pliocene boundary falls between Sample 975B-33X-2, 132–134 cm, and Sample 33X-2, 130–132 cm, at 305.23 mbsf, corresponding to a lithologic and color change (Fig. 4). The CaCO_3 curve shows a strange pattern; in fact, the uppermost Messinian sediments are richer in CaCO_3 than the lowermost Pliocene sediments (Fig. 5). Small clasts dispersed in the pelagic ooze characterize the very base of the Pliocene sediments (Fig. 6). Planktonic foraminifers are abundant, well preserved, and well diversified from the base of the Pliocene sediments (Table 4 and Appendix C).

The major events recognized within Zone MP11 are the following:

1. The FCO of *Gr. margaritae* marking the base of MP12, at Sample 161-975B-32X-3, 116–118 cm (at 296.81 mbsf);
2. The acme interval of *Sphaeroidinellopsis* (2.6 m thick) between Sample 161-975B-33X-2, 0–2 cm, and Sample 32X-6, 116–118 cm;
3. Two sinistral shifts of *N. acostaensis*, the lower one from Sample 161-975B-33X-2, 50–52 cm (at 304.41 mbsf) up to 33X-2, 30–32 cm (at 304.21 mbsf) and the higher one from Sample 975B-33X-1, 143–145 cm (at 303.84 mbsf) up to 33X-1, 117–119 cm (at 303.58 mbsf) for a thickness of 0.20 m and 0.26 m respectively;
4. The CO of *Gr. scitula* dextral occurs from Sample 161-975B-33X-1, 125–127 cm, at 303.66 mbsf, which is 1.5 m above the Miocene/Pliocene boundary; and
5. A peak of abundance (9.2%) of *Gg. nepenthes* at Sample 161-975B-33X-2, 10–12 cm, at 304.01 mbsf just below the base of the *Sphaeroidinellopsis* acme interval.

Total benthic foraminifers from the fraction $>125 \mu\text{m}$ is shown in Appendix D; only semi-quantitative analyses were conducted for the fraction $<125 \mu\text{m}$.

The interval studied is characterized by the following benthic “events”:

1. The uppermost Messinian is characterized by the abundance of *Bolivina* cf. *paralica*, *Rosalina* spp., and small *Ammonia tepida* (Iaccarino and Bossio, Chap. 42, this volume);
2. At the base of MP11 Zone, *Brizalina-Bolivina* gr. and *Trifarina bradyi* are present and *G. gr. soldanii* and *Oridorsalis umbonatus* show the highest abundances. At the very base (Samples 161-975B-33X-2, 130–132 cm, to 33X-2, 116–118 cm) *Eponides pusillus* and *Epistominella exigua* are common in the fraction $<125 \mu\text{m}$;
3. At 304.41 mbsf (Sample 161-975B-33X-2, 50–52 cm) *G. subglobosa* becomes one of the dominant taxa;
4. At about 304 mbsf (Samples 161-975B-33X-2, 20–22 cm, and 33X-2, 10–12 cm) *O. stellatus* and the agglutinants (mainly represented by *K. bradyi*, *Martinottiella* spp., and *Bigenerina nodosaria*) first occur and/or become more abundant;
5. From 303.16 mbsf (Sample 161-975B-33X-1, 75–77 cm) a high benthic abundance is recorded; *G. subglobosa* shows increasing percentages, and *Uvigerina* spp. becomes continuously present with low percentages; and
6. At 302.39 mbsf (Sample 161-975B-32X-CC, 37–39 cm) *Uvigerina pygmaea-peregrina* increases, and a sharp decrease of *G. subglobosa* occurs.

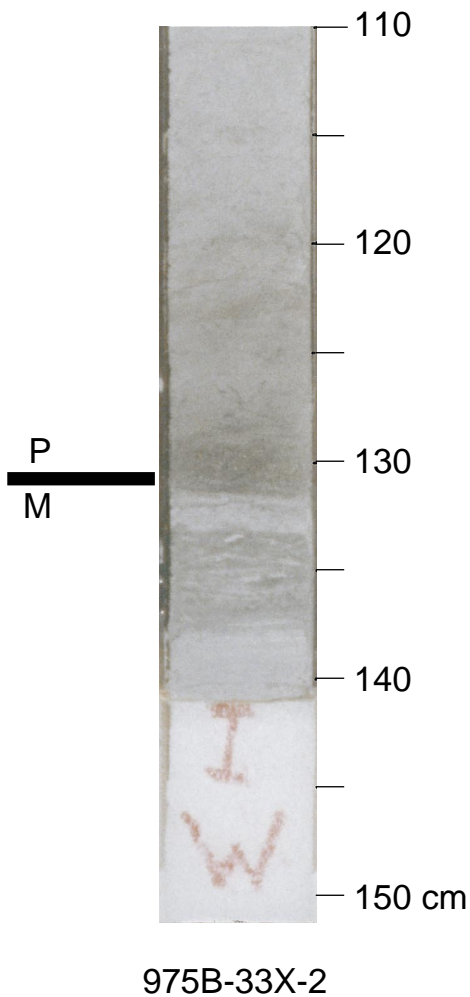


Figure 4. Lithologic variation at Miocene/Pliocene boundary in Hole 975B. The boundary falls at Sample 161-975B-33X-2, 132 cm, between gray and whitish color change.

come continuous. Sgarrella et al. (1997) recognized this event in the Jonian Basin starting from Cycle 4.

According to McKenzie and Sprovieri (1990) and Sprovieri and Hasegawa (1990), a low oxygen content characterizes the bottom waters of the Mediterranean Basin in the basal part of Zone MP11. However, the distribution of the benthic foraminifers sensitive to oxygen content shows variations that are not simultaneous in the Tyrrhenian and Balearic Basins, probably because of the different depths and physiographies of the two basins.

CONCLUSIONS

The basal Pliocene sediments are typical pelagic oozes composed mainly of planktonic foraminifers. At Site 975, however, in the first 2–3 cm of the Pliocene sediments, small clasts are present within the pelagic ooze, indicating terrigenous input. The benthic population indicates that at the beginning of the Pliocene, circulation was restricted in Hole 974B and was disaerobic in Hole 975B. Only later, when the connection with the Atlantic Ocean was well established, did the benthic fauna increase and become more diversified.

The paleoenvironmental change at the Miocene/Pliocene boundary is also recognizable through the lithology (mainly in Hole 975B) and carbonate content (mainly in Hole 974B).

The sedimentation rate was higher in Hole 974B than in Hole 975B and was constant for the entire Zone MP11 (Fig. 11). The Miocene/Pliocene boundary is identifiable at both sites (no more than 0.2 k.y. are missing in Hole 974B) and correlates with that of the Capo Rossello composite section, which is five cycles below the Thvera Subchron. In fact, even if the paleomagnetic data are not available for these sequences, the position of the polarity change may be inferred through the biostratigraphic events and the *Globigerinoides* fluctuations related to the precession periodicity (Fig. 12).

ACKNOWLEDGMENTS

We are grateful to Dr. R.H. Benson and Dr. W.J. Zachariasse for the critical review of the paper.

REFERENCES

- Berggren, W.A., Hilgen, F.J., Langereis, C.G., Kent, D.V., Obradovich, J.D., Raffi, I., Raymo, M.E., and Shackleton, N.J., 1995. Late Neogene chronology: new perspectives in high-resolution stratigraphy. *Geol. Soc. Am. Bull.*, 107:1272–1287.
- Caralp, M., Moyes, J., and Vigneaux, M., 1970. Essai d'utilisation des mélanges de microorganismes benthiques dans la reconstitution des environnements. Application à un canyon du Golfe de Gascogne. *Deep-Sea Res.*, 17:661–670.
- Cita, M.B., 1973. Pliocene biostratigraphy and chronostratigraphy. In Ryan, W.B.F., Hsu, K.J., et al., *Init. Repts. DSDP*, 13 (Pt. 2): Washington (U.S. Govt. Printing Office), 1343–1379.
- , 1975. Studi sul Pliocene e gli strati di passaggio dal Miocene al Pliocene, VII. Planktonic foraminiferal biozonation of the Mediterranean Pliocene deep sea record: a revision. *Riv. Ital. Paleontol. Stratigr.*, 81:527–544.
- Cita, M.B., Wright, R.C., Ryan, W.B.F., and Longinelli, A., 1978. Messinian paleoenvironments. In Hsu, K.J., Montadert, L., et al., *Init. Repts. DSDP*, 42 (Pt. 1): Washington (U.S. Govt. Printing Office), 1003–1035.
- Di Stefano, E., Sprovieri, R., and Scarantino, S., 1996. Chronology of biostratigraphic events at the base of the Pliocene. *Paleopelagos*, 6:401–414.
- Hasegawa, S., Sprovieri, R., and Poluzzi, A., 1990. Quantitative analyses of benthic foraminiferal assemblages from Plio-Pleistocene sequences in the Tyrrhenian Sea, ODP Leg 107. In Kastens, K.A., Mascle, J., et al., 1990. *Proc. ODP, Sci. Results*, 107: College Station, TX (Ocean Drilling Program), 461–478.
- Hilgen, F.J., 1991. Extension of the astronomically calibrated (polarity) time scale to the Miocene/Pliocene boundary. *Earth Planet. Sci. Lett.*, 107:349–368.
- Hsu, K.J., Montadert, L., Bernoulli, D., Cita, M.B., Erickson, A., Garrison, R.E., Kidd, R.B., Melières, F., Müller, C., and Wright, R., 1978. History of the Mediterranean salinity crisis. In Hsu, K.J., Montadert, L., et al., *Init. Repts. DSDP*, 42 (Pt. 1): Washington (U.S. Govt. Printing Office), 1053–1078.
- Iaccarino, S., 1985. Mediterranean Miocene and Pliocene planktic foraminifera. In Bolli, H.M., Saunders, J.B., and Perch-Nielsen, K. (Eds.), *Plankton Stratigraphy*: Cambridge (Cambridge Univ. Press), 283–314.
- Langereis, C.G., and Hilgen, F.J., 1991. The Capo Rossello composite: a Mediterranean and global reference section for the early to early-late Pliocene. *Earth Planet. Sci. Lett.*, 104:211–225.
- Lohman, G.P., 1978. Abyssal bentonic foraminifera as hydrographic indicators in the western south Atlantic Ocean. *J. Foraminiferal. Res.*, 8:6–34.
- McKenzie, J.A., and Sprovieri, R., 1990. Paleoceanographic conditions following the earliest Pliocene flooding of the Tyrrhenian Sea. In Kastens, K.A., Mascle, J., et al., *Proc. ODP, Sci. Results*, 107: College Station, TX (Ocean Drilling Program), 405–414.
- Mullineaux, L.S., and Lohman, G.P., 1981. Late Quaternary stagnation and recirculation of the eastern Mediterranean. *J. Foraminiferal. Res.*, 11:20–39.

- Rio, D., Sprovieri, R., and Raffi, I., 1984. Calcareous plankton biostratigraphy and biochronology of the Pliocene-lower Pleistocene succession of the Capo Rossello area (Sicily). *Mar. Micropaleontol.*, 9:135–180.
- Ryan, W.B.F., Hsü, K.J., et al., 1973. *Init. Repts. DSDP*, 13 (Pts. 1 and 2): Washington (U.S. Govt. Printing Office).
- Sgarrella, F., Sprovieri, R., Di Stefano, E., and Caruso, A., 1997. Paleoceanographic conditions at the base of the Pliocene in the southern Mediterranean basin. *Riv. Ital. Paleontol. Stratigr.*, 103:207–220.
- Shipboard Scientific Party, 1996a. Site 974. In Comas, M.C., Zahn, R., Klaus, A., et al., *Proc. ODP, Init. Repts.*, 161: College Station, TX (Ocean Drilling Program), 55–111.
- _____, 1996b. Site 975. In Comas, M.C., Zahn, R., Klaus, A., et al., *Proc. ODP, Init. Repts.*, 161: College Station, TX (Ocean Drilling Program), 113–177.
- Smart, C.W., King, S.C., Gooday, A.J., Murray, J.W., and Thomas, E., 1994. A benthic foraminiferal proxy of pulsed organic matter paleofluxes. *Mar. Micropaleontol.*, 23:89–99.
- Sprovieri, R., 1992. Mediterranean Pliocene biochronology: a high resolution record based on quantitative planktonic foraminifera distribution. *Riv. Ital. Paleontol. Stratigr.*, 98:61–100.
- _____, 1993. Pliocene–early Pleistocene astronomically forced planktonic foraminifera abundance fluctuations and chronology of Mediterranean calcareous plankton bio-events. *Riv. Ital. Paleontol. Stratigr.*, 99:371–414.
- Sprovieri, R., Di Stefano, E., Caruso, A., and Bonomo, S., 1996. High resolution stratigraphy in the Messinian Tripoli Formation in Sicily. *Paleopelagos*, 6:415–435.
- Sprovieri, R., and Hasegawa, S., 1990. Plio-Pleistocene benthic foraminifer stratigraphic distribution in the deep-sea record of the Tyrrhenian Sea (ODP Leg 107). In Kastens, K.A., Mascle, J., et al., *Proc. ODP, Sci. Results*, 107: College Station, TX (Ocean Drilling Program), 429–459.
- Van der Zwaan, G.J., 1982. Paleoecology of Late Miocene Mediterranean foraminifera. *Utrecht Micropaleontol. Bull.*, 25:1–202.
- Vismara Schilling, A., 1986. Foraminiferi bentonici profondi associati ad eventi anossici del Pleistocene medio e superiore nel Mediterraneo orientale. *Riv. Ital. Paleonteontol. Stratigr.*, 92:103–148.
- Zachariasse, W.J., and Spaak, P., 1983. Middle Miocene to Pliocene paleoenvironmental reconstructions of the Mediterranean and adjacent Atlantic Ocean: planktonic foraminiferal records of southern Italy. *Utrecht Micropaleontol. Bull.*, 30:91–110.

Date of initial receipt: 9 May 1997

Date of acceptance: 14 October 1997

Ms 161SR-247

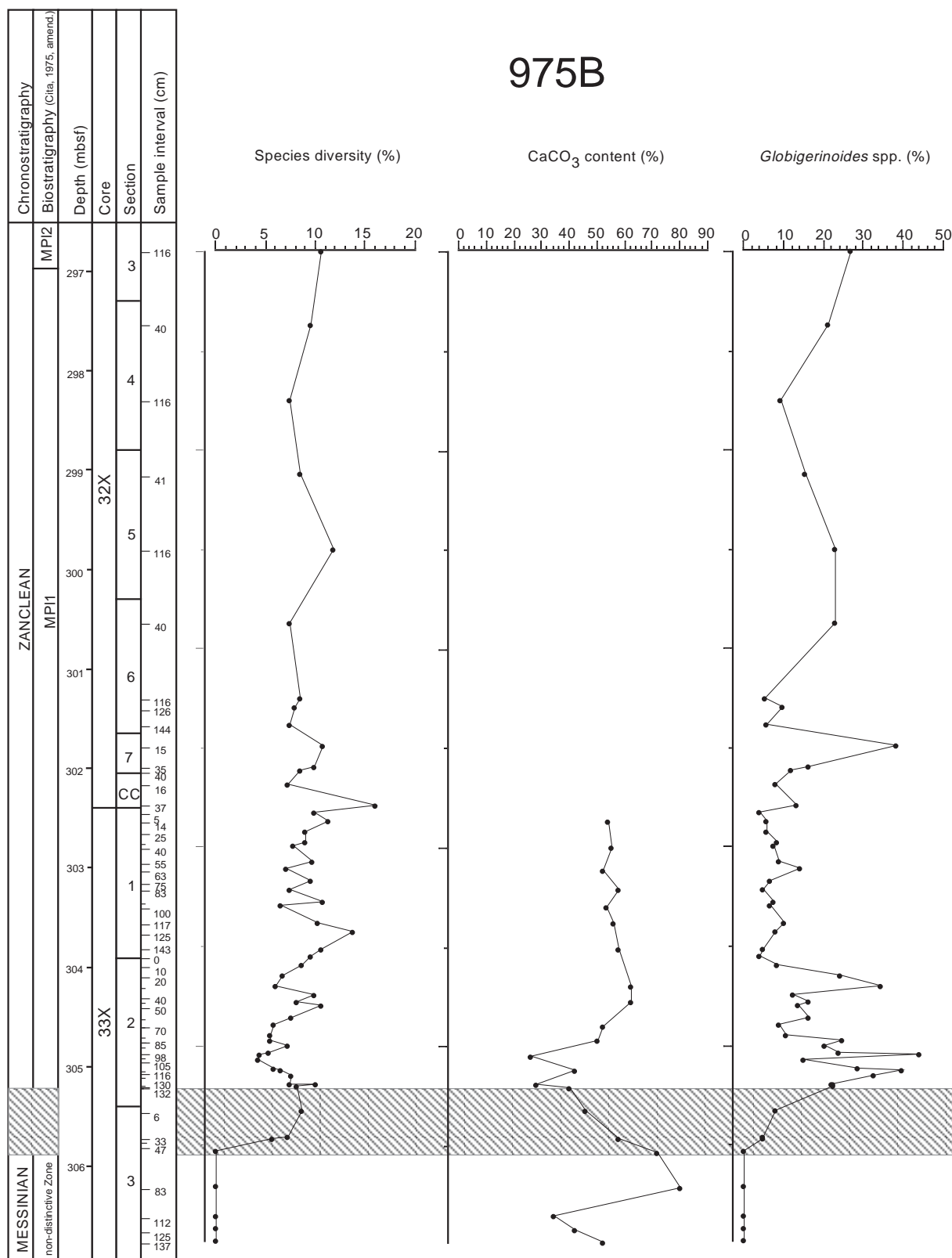


Figure 5. Specific diversity of planktonic foraminifers, CaCO₃, and *Globigerinoides* spp. curves in Hole 975B. The shadow area below the M/P boundary corresponds to a transitional unit at the top of the Messinian sequence. The CaCO₃ curve is based on a minor number of samples in respect to the *Globigerinoides* curve.

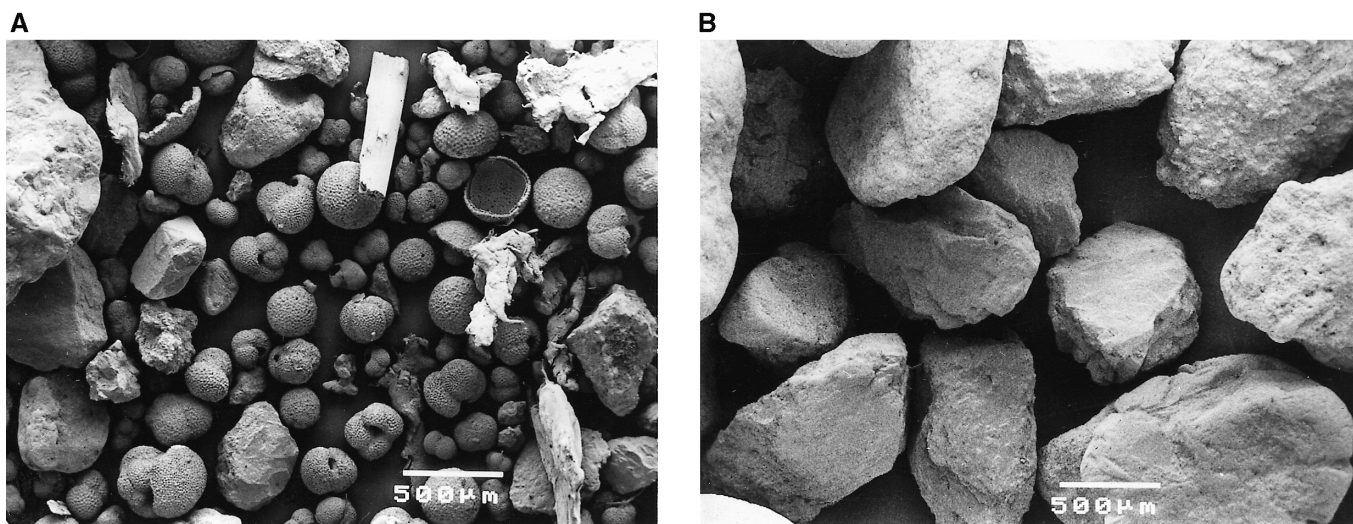


Figure 6. Residue composition in Sample 161-975B-33X-2, 129–131 cm, in two different fractions. **A.** Fraction $> 125 \mu\text{m}$: planktonic foraminifera are associated with clasts. **B.** Fraction $> 300 \mu\text{m}$.

Table 4. Percentages of selected planktonic foraminifers in Hole 975B.

| Core, section, interval (cm) | <i>Gr. margaritae</i> | <i>Ss. seminudina</i> | <i>N. acostaensis</i> (sx) | <i>N. acostaensis</i> (dx) | <i>Gr. scitula</i> (dx) | <i>Gr. scitula</i> (sx) | <i>Gg. nepenthes</i> |
|---------------------------------|-----------------------|-----------------------|----------------------------|----------------------------|-------------------------|-------------------------|----------------------|
| 161-975B- | | | | | | | |
| 32X-3, 116-118 | 8.5 | 0.4 | 12.0 | | | | |
| 32X-4, 40-42 | | 0.7 | 9.9 | 0.7 | | 0.3 | |
| 32X-4, 116-118 | | 1.2 | 0.6 | 23.3 | 1.5 | 0.3 | 0.9 |
| 32X-5, 41-43 | | 0.5 | | 16.4 | 0.3 | | 1.6 |
| 32X-5, 116-118 | | | | 16.4 | 8.5 | | 0.3 |
| 32X-6, 40-42 | | | 0.7 | 14.7 | | | 2.4 |
| 32X-6, 116-118 | | 0.6 | 0.3 | 16.6 | 7.2 | 1.6 | 1.6 |
| 32X-6, 126-128 | | 0.5 | 0.5 | 13.8 | 9.2 | 0.2 | 1.6 |
| 32X-6, 144-146 | | 1.9 | 0.5 | 12.0 | 1.6 | | 2.2 |
| 32X-7, 15-17 | | 1.4 | | 13.1 | 1.8 | 0.7 | 2.5 |
| 32X-7, 35-37 | | 0.3 | 0.9 | 16.3 | 0.6 | | 0.3 |
| 32X-7, 40-42 | | 1.7 | 1.1 | 16.9 | 2.9 | | 4.0 |
| 32X-CC, 16-18 | | 0.9 | 2.1 | 30.3 | 0.9 | 0.3 | 4.0 |
| 32X-CC, 37-39 | | 1.8 | | 10.8 | 4.8 | 0.6 | 2.7 |
| 33X-1, 5-7 | | | | 17.6 | 2.2 | 0.9 | 2.8 |
| 33X-1, 14-16 | | 1.2 | 0.9 | 13.2 | 6.1 | 0.6 | 0.9 |
| 33X-1, 25-27 | | 2.9 | 1.0 | 9.6 | | | 3.8 |
| 33X-1, 35-37 | | 0.7 | 1.0 | 7.8 | | | 7.8 |
| 33X-1, 40-42 | | 0.6 | 1.8 | 16.7 | 0.9 | | 2.3 |
| 33X-1, 55-57 | | 1.0 | 1.0 | 17.3 | 1.0 | | 5.9 |
| 33X-1, 63-65 | | 0.8 | 1.9 | 21.7 | 1.4 | 0.3 | 0.5 |
| 33X-1, 75-77 | | 0.9 | 0.6 | 22.2 | 0.3 | 0.3 | 1.5 |
| 33X-1, 83-85 | | 0.9 | 0.9 | 12.8 | 0.3 | | 0.6 |
| 33X-1, 95-97 | | 0.5 | 2.4 | 17.3 | 3.2 | | 4.4 |
| 33X-1, 100-102 | | 0.9 | 1.2 | 12.2 | 1.5 | | 4.5 |
| 33X-1, 117-119 | | 1.1 | 5.2 | 10.6 | 2.6 | | 3.2 |
| 33X-1, 125-127 | | 2.3 | 6.8 | 6.0 | 3.7 | | 3.7 |
| 33X-1, 143-145 | | 3.4 | 12.7 | 5.2 | 0.3 | | 1.2 |
| 33X-2, 0-2 | | 1.9 | 4.1 | 22.5 | 0.6 | | 4.4 |
| 33X-2, 10-12 | | | 2.0 | 19.6 | 0.3 | | 9.2 |
| 33X-2, 20-22 | | | 0.3 | 15.4 | 0.9 | | 4.2 |
| 33X-2, 30-32 | | 0.3 | 2.4 | 12.7 | | | 1.2 |
| 33X-2, 40-42 | | 0.9 | 14.2 | 3.6 | 0.3 | | 7.4 |
| 33X-2, 46-48 | | 0.3 | 17.9 | 3.5 | | | 1.9 |
| 33X-2, 50-52 | | | 14.3 | 3.7 | 2.2 | | 6.8 |
| 33X-2, 62-64 | | 0.5 | | 26.1 | 0.3 | 0.3 | 4.0 |
| 33X-2, 70-72 | | | 0.3 | 20.5 | 1.0 | | 2.9 |
| 33X-2, 80-82 | | | 1.3 | 15.8 | 2.3 | | 3.9 |
| 33X-2, 85-87 | | | | 13.9 | | 0.3 | 2.2 |
| 33X-2, 90-92 | | | 1.2 | 16.4 | | | 6.1 |
| 33X-2, 98-100 | | | 0.6 | 17.0 | | | 5.0 |
| 33X-2, 100-102 | | | 1.3 | 6.9 | 0.3 | | 1.6 |
| 33X-2, 105-107 | | | | 16.8 | | 0.3 | 1.6 |
| 33X-2, 114-116 | | | 0.6 | 7.1 | | | 7.3 |
| 33X-2, 116-118 | | | | 6.8 | | | 5.6 |
| 33X-2, 120-122 | | 0.5 | 0.3 | 2.9 | | 0.3 | 5.5 |
| 33X-2, 129-131 | | | 0.3 | 11.0 | 0.3 | 0.3 | 0.9 |
| 33X-2, 130-132 | | | 0.8 | 4.8 | 0.8 | 0.8 | 2.7 |
| 33X-2, 132-134 | | 0.6 | 0.6 | 7.0 | | 0.6 | 1.3 |
| 33X-3, 6-8 | c | 0.3 | 1.2 | 18.1 | 2.3 | | 2.9 |
| 33X-3, 33-35 | c | | 0.8 | 12.8 | 1.0 | 0.5 | 4.8 |
| 33X-3, 35-37 | c | 0.2 | 1.3 | 13.2 | 0.6 | | 5.0 |
| 33X-3, 47-49 | | | | | | | |
| 33X-3, 83-85 | | | | | | | |
| 33X-3, 112-114 | | | | | | | |
| 33X-3, 125-127 | | | | | | | |
| 33X-3, 137-139 | | | | | | | |

Note: c = downhole contamination; blank space = planktonic foraminifers absent.

Table 5. Depth and age of the events and cycles in Hole 974B.

| Events | Depth (mbsf) | Age (Ma) |
|--------------------------------------|-----------------|-------------|
| FCO <i>Gr. margaritae</i> | 296.8 | 5.07 |
| Top <i>Sphaeroidinellopsis</i> acme | 301.6 | 5.20 |
| Top Cycle 6 | 301.41 | |
| Top Cycle 5 | 302.18 | |
| Top Cycle 4 | 302.5 | |
| Top Cycle 3 | 303.3 | |
| Base <i>Sphaeroidinellopsis</i> acme | 303.9 | 5.29 |
| Top Cycle 2 | 303.9 | |
| Top Cycle 1 | 304.5 | |
| Base Pliocene | 305.21 | 5.33 |

Table 6. Depth and age of the events and cycles in Hole 975B.

| Events | Depth (mbsf) | Age (Ma) |
|--------------------------------------|-----------------|-------------|
| FCO <i>Gr. margaritae</i> | 183.06 | 5.07 |
| Top <i>Sphaeroidinellopsis</i> acme | 190.80 | 5.20 |
| Top Cycle 6 | 191.03 | |
| Top Cycle 5 | 193.40 | |
| Top Cycle 4 | 194.30 | |
| Top Cycle 3 | 196.37 | |
| Base <i>Sphaeroidinellopsis</i> acme | 197.90 | |
| | 198.00 | 5.29 |

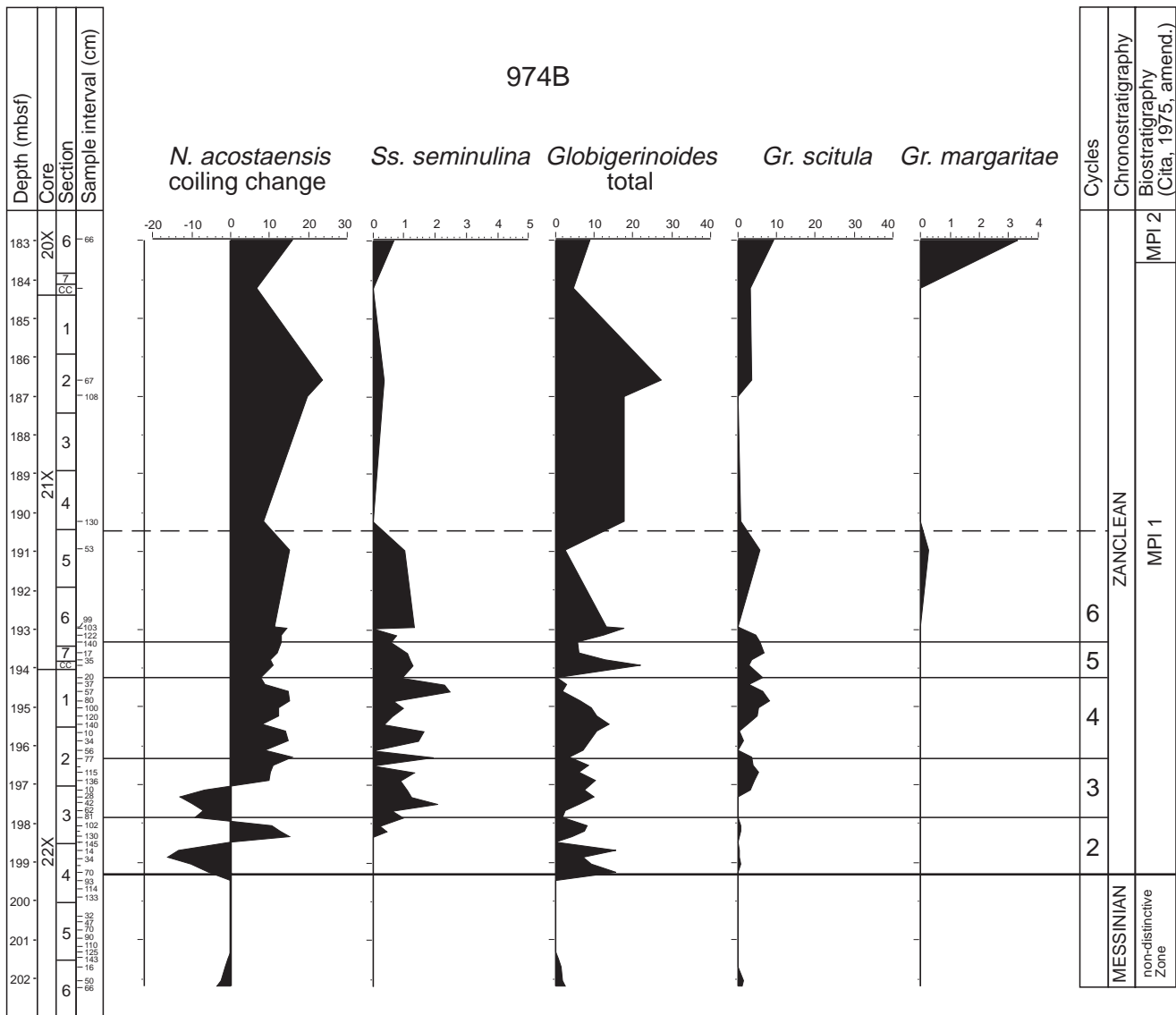


Figure 7. Events and abundance curves (%) of the most significant planktonic foraminifers in Hole 974B. Precession cycles listed on the right are well recognizable from Cycle 2 to Cycle 6. The upper boundary of Cycle 6 is dashed because the sampling is too loose in this interval and the boundary could be located above. Cycle 1 is missing.

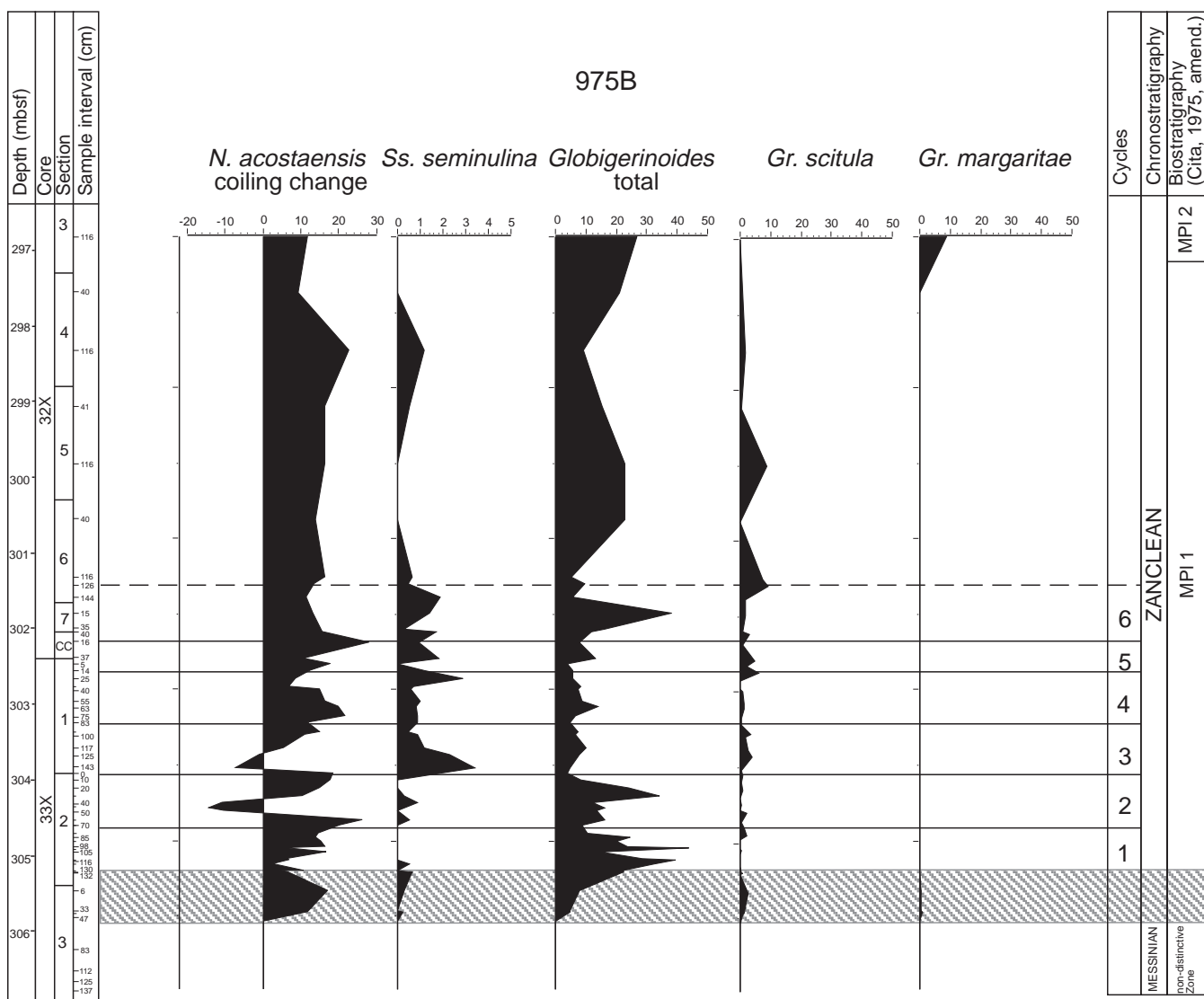


Figure 8. Events and abundance curves (%) of the most significant planktonic foraminifers in Hole 975B. Precession cycles listed on the right are well recognizable from Cycle 1 to Cycle 6. The upper boundary of Cycle 6 is dashed because the sampling is too loose in this interval and the boundary could be located above. The shadow area below the M/P boundary corresponds to a transitional unit at the top of the Messinian sequence.

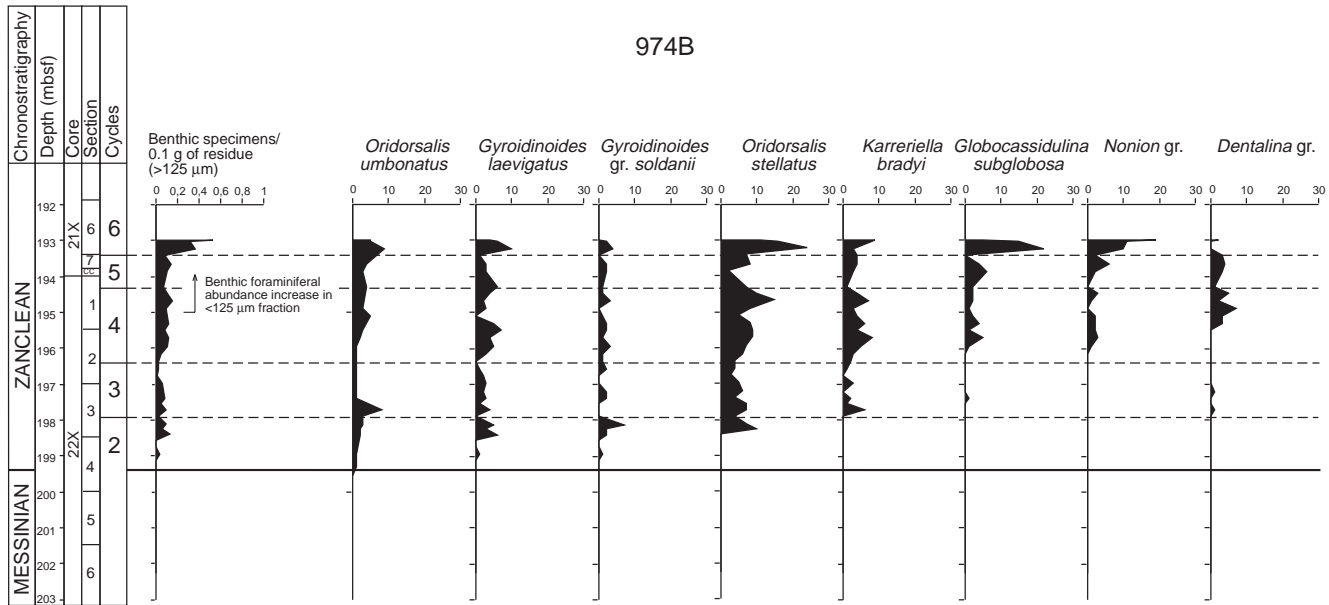


Figure 9. Quantitative distribution curves of benthic foraminifers vs. cycles in Hole 974B (see Appendix E).

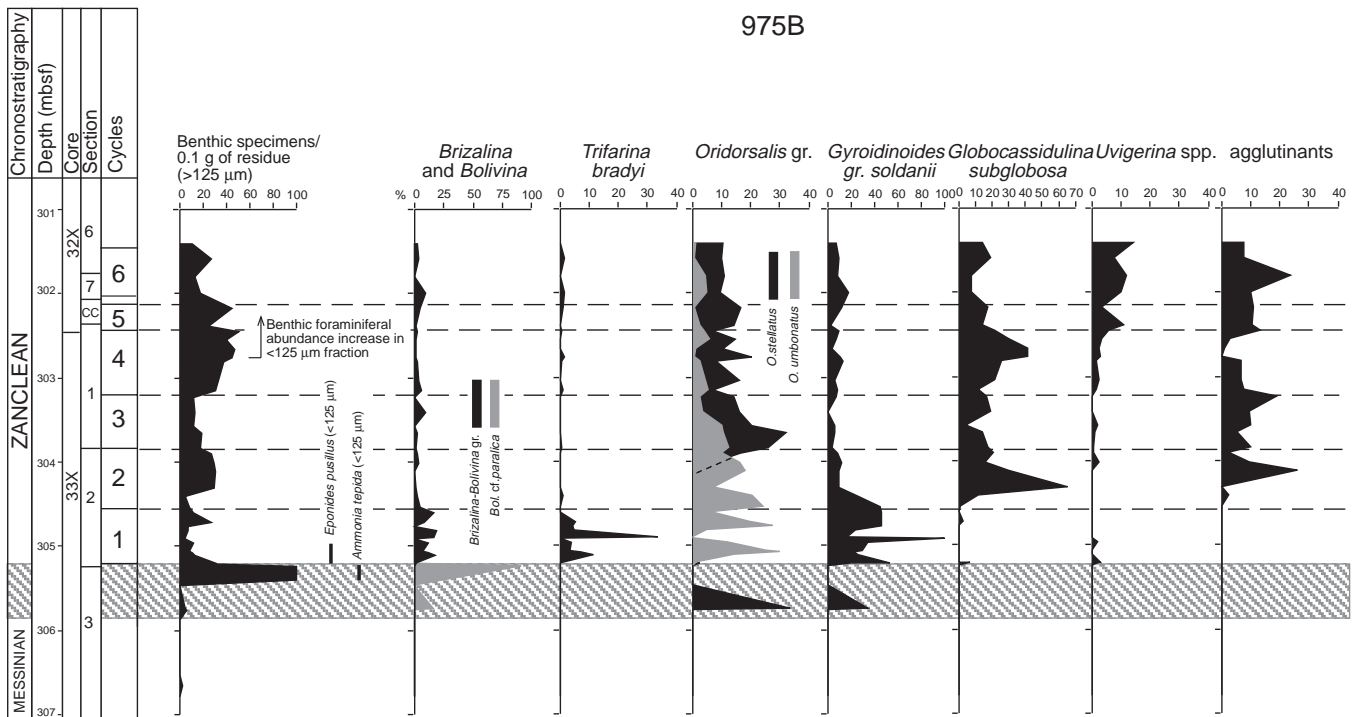


Figure 10. Frequency curves (%) of benthic foraminifers vs. cycles in Hole 975B (see Appendix E). The shaded area below the M/P boundary corresponds to a transitional unit at the top of the Messinian sequence.

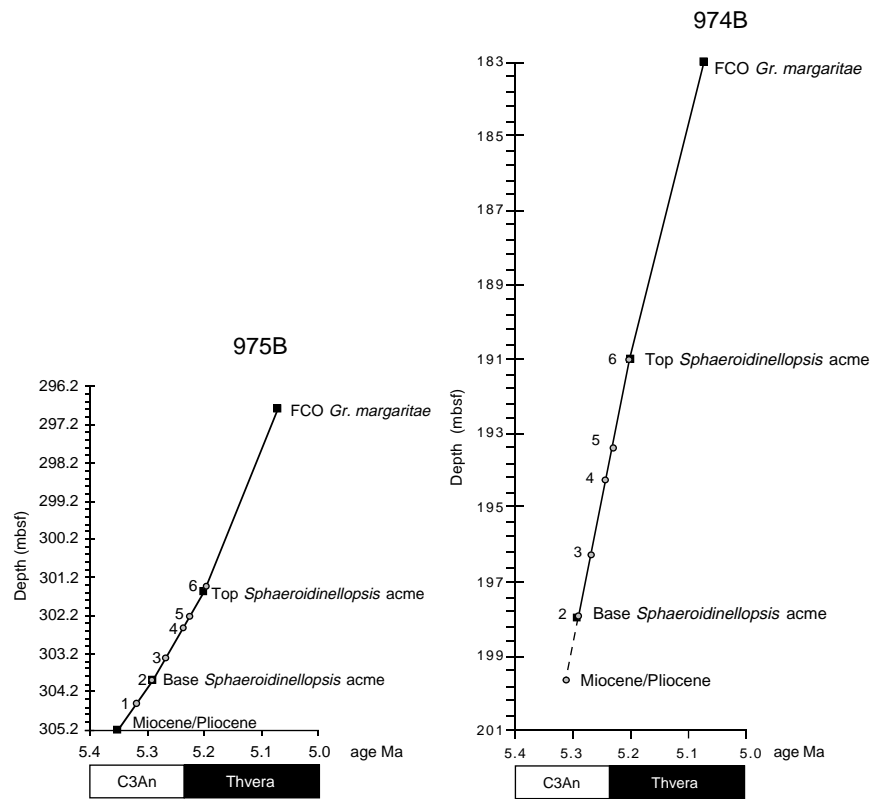


Figure 11. Age (Hilgen, 1991; Berggren et al., 1995) vs. depth of the cycles and biostratigraphic events in Zone MP11. The sedimentation rate is higher in Hole 974B than in Hole 975B, but the difference remains constant through the entire interval. Circles indicate the top depths of the cycles; squares indicate the bio-events.

974B

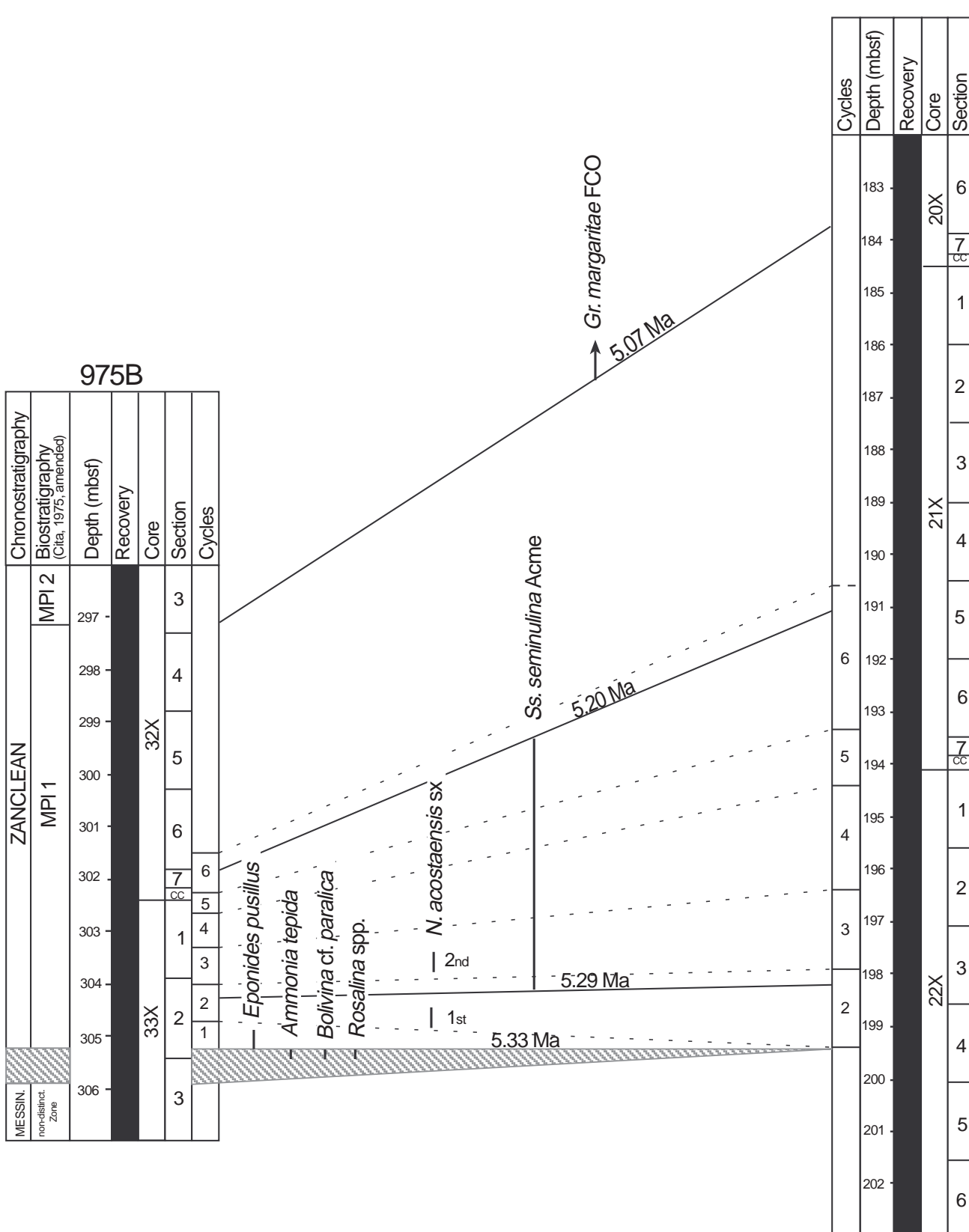


Figure 12. Comparison between the major biostratigraphic events and cycles within the two holes. The shaded area below the M/P boundary corresponds to a transitional unit at the top of the Messinian sequence.

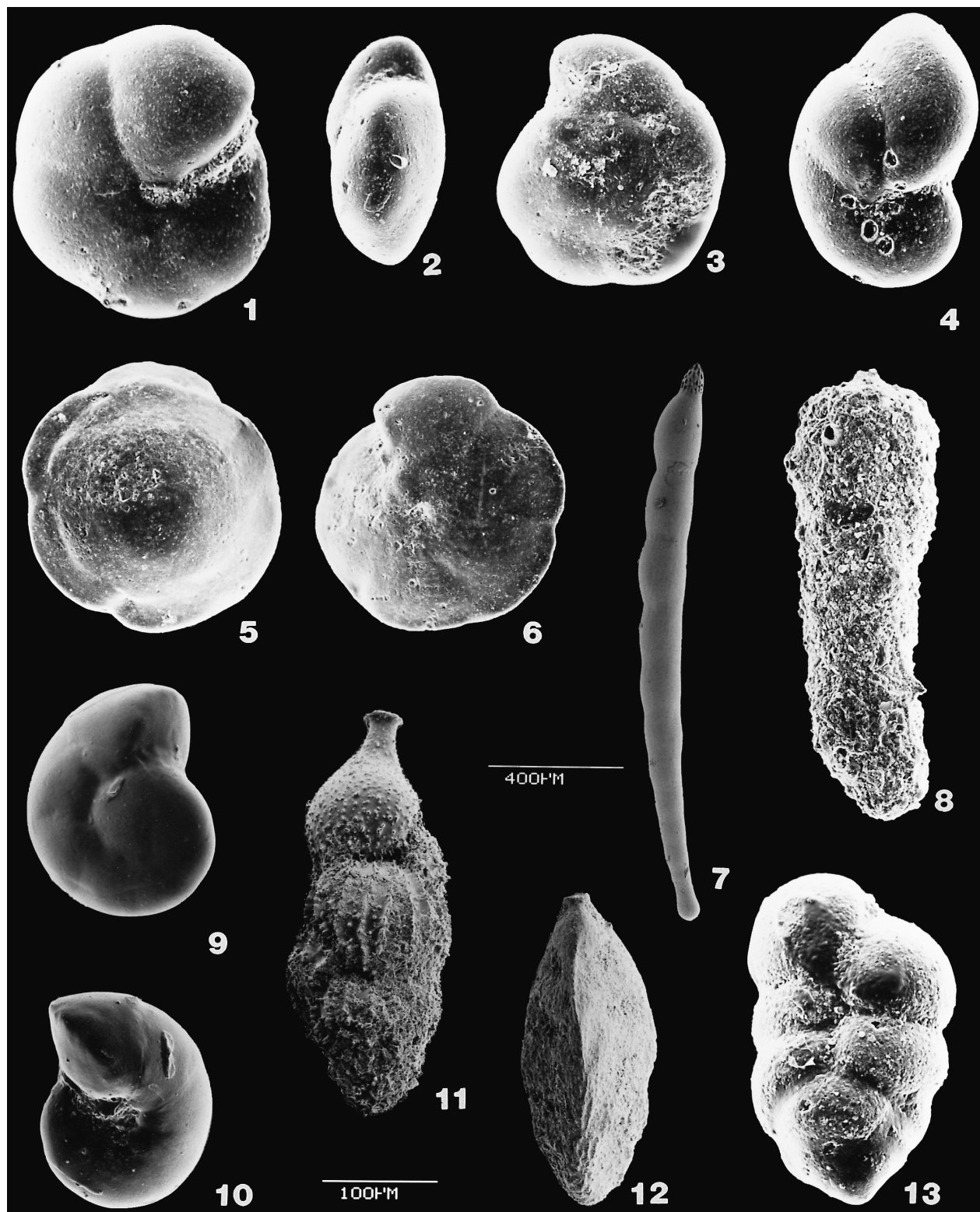


Plate 1. **1–3.** *Oridorsalis umbonatus* (Reuss). Sample 161-975B-33X-2, 0–2 cm. **4.** *Nonion* sp. Sample 161-974B-21X-2, 108–110 cm. **5, 6.** *Oridorsalis stellatus* (Silvestri). Sample 161-975B-33X-2, 0–2 cm. **7.** *Dentalina filiformis* (d'Orbigny). Sample 161-974B-22X-1, 37–39 cm. **8.** *Martinottiella communis* (d'Orbigny). Sample 161-975B-33X-2, 0–2 cm. **9, 10.** *Gyroidinoides laevigatus* (d'Orbigny). Sample 161-974B-22X-1, 80–82 cm. **11.** *Uvigerina pygmaea* d'Orbigny. Sample 161-974B-21X-5, 53–55 cm. **12.** *Trifarina bradyi* Cushman. Sample 161-975B-33X-2, 120–122 cm. **13.** *Karreriella bradyi* (Cushman). Sample 161-974B-22X-1, 80–82 cm. The larger magnification (400 μ m) refers to figure 7 only.

Appendix B. Quantitative range chart of benthic foraminifers (>125 µm) through the Miocene/Pliocene boundary and MP11 Zone in Hole 974B.

| Core, section, interval (cm) | Total benthic foraminifers | | | | | | | | | | | | | | | | | |
|------------------------------|------------------------------|--|--|--|--|--|-------------------------------------|---------------------------|--|--|--|--|---------------------------------|----------------------------|--|--|--|--|
| | <i>Oridorsalis umbonatus</i> | | | | | | <i>Gyroidinoides gr. soldanii</i> * | | | | | | <i>Gyroidinoides laevigatus</i> | | | | | |
| | | | | | | | | <i>Pulenia salisburyi</i> | | | | | | <i>Silostomella</i> spp. * | | | | |
| | | | | | | | | | <i>Cibicidoides unglerianus</i> | | | | | | | | | |
| | | | | | | | | | <i>Globosepta charoides</i> | | | | | | | | | |
| | | | | | | | | | <i>Oridorsalis stellaris</i> | | | | | | | | | |
| | | | | | | | | | <i>Dentalina filiformis</i> | | | | | | | | | |
| | | | | | | | | | <i>Karreniella bradyi</i> | | | | | | | | | |
| | | | | | | | | | <i>Martinottiella communis</i> | | | | | | | | | |
| | | | | | | | | | <i>Globocassidulina subglobosa</i> | | | | | | | | | |
| | | | | | | | | | <i>Quinqueloculina</i> spp. | | | | | | | | | |
| | | | | | | | | | <i>Cibicidoides pseudoungerianus</i> | | | | | | | | | |
| | | | | | | | | | <i>Eggerella bradyi</i> | | | | | | | | | |
| | | | | | | | | | <i>Uvigerina</i> spp. * | | | | | | | | | |
| | | | | | | | | | <i>Cibicides refugens</i> | | | | | | | | | |
| | | | | | | | | | <i>Nonion</i> gr. * | | | | | | | | | |
| | | | | | | | | | <i>Nodosaria</i> spp. * | | | | | | | | | |
| | | | | | | | | | <i>Dentalina</i> sp. | | | | | | | | | |
| | | | | | | | | | <i>Furcicarinina squammosa</i> | | | | | | | | | |
| | | | | | | | | | <i>Brizalina-Bivalvina</i> gr. * | | | | | | | | | |
| | | | | | | | | | <i>Cibicides lobatulus</i> | | | | | | | | | |
| | | | | | | | | | <i>Elphidium complanatum</i> | | | | | | | | | |
| | | | | | | | | | <i>Marginulina subbulata</i> | | | | | | | | | |
| | | | | | | | | | <i>Pleurostomella alternans</i> | | | | | | | | | |
| | | | | | | | | | <i>Triloculina</i> sp. | | | | | | | | | |
| | | | | | | | | | <i>Globobulimina saubrigensis</i> | | | | | | | | | |
| | | | | | | | | | <i>Lagenia</i> spp. * | | | | | | | | | |
| | | | | | | | | | <i>Sigmoilinita tenuis</i> | | | | | | | | | |
| | | | | | | | | | <i>Dinormorpha tuberosa</i> | | | | | | | | | |
| | | | | | | | | | <i>Chrysogonium lanceolum</i> | | | | | | | | | |
| | | | | | | | | | <i>Astromenion stelligerum</i> | | | | | | | | | |
| | | | | | | | | | <i>Quadrimorphina allomorphinoides</i> | | | | | | | | | |
| | | | | | | | | | <i>Uvigerina pigrina-peregrina</i> | | | | | | | | | |
| | | | | | | | | | <i>Anomalioidea elutianensis</i> | | | | | | | | | |
| | | | | | | | | | <i>Globocassidulina oblonga</i> | | | | | | | | | |
| | | | | | | | | | <i>Oriomorphina cf. tenuicostata</i> | | | | | | | | | |
| | | | | | | | | | <i>Globulina gibba</i> | | | | | | | | | |
| | | | | | | | | | Indet. specimens | | | | | | | | | |

Note: * = groupings of species (see Appendix E); blank space = benthic foraminifers absent.

Appendix E

In Appendixes B and D some species of benthic foraminifers were grouped because of their very rare and scattered presence:

Anomalinoidea alazanensis: comprises also *A. alazanensis spissiformis*.

Amphicoryna spp.: includes *A. scalaris*, *A. semicostata*, and *A. sublineata*.

Brizalina and *Bolivina*: in Hole 975B, *Brizalina-Bolivina* gr. includes many species having a generally scattered distribution: *Bolivina alazanensis*, *B. cf. suteri*, *B. cistica*, *B. fastigia*, *B. lanceolata*, *B. leonardii*, *B. punctata*, *B. reticulata*, *Bolivinita quadrilatera*, *Brizalina arta*, *Br. catanensis*, *Br. dilatata*, *Br. spathulata*, *Br. dinopolii*, *Br. lanceolata*, *Brizalina* spp. In Hole 974B, *B. leonardii*, *Br. dinopolii*, and *Brizalina* sp. were found in Cycle 4.

Cassidulina spp.: this genus is represented mainly by *C. neocarinata* and, rarely, by *C. laevigata*.

Chrysogonium spp.: includes *C. lanceolum*, *C. tenuicostatum* and *C. cf. obliquatum*.

Dentalina spp.: comprises *D. aciculata*, *D. cuvieri*, *D. inornata*, and some unidentified specimens; the most common species *D. filiformis* and *D. leguminiformis* were not grouped.

Elphidium spp.: includes *E. advenum* and *E. complanatum*.

Fissurina spp.: comprises *F. apiculata*, *F. bradyiana*, *F. marginata*, *F. orbignyana*, *F. pseudorbignyana*, and some unidentified specimens.

Gyroidinoides gr. *soldanii*: this group includes *G. soldanii* and *G. neosoldanii* in both holes.

Gyroidinoides spp.: groups *G. girardanus*, *G. umbonatus*, and some unidentified forms.

Lagena spp.: in Hole 975B it includes *L. sulcata interrupta*, *L. tenuistriatiformis*, and some unidentified specimens; in Hole 974B, includes two unidentified specimens.

Lenticulina spp.: groups *L. cf. brevispinosa*, *L. gibba*, *L. peregrina*, *L. stellata*, and some unidentified specimens.

Marginulina spp.: includes *M. glabra*, *M. subbulata*, and some unidentified specimens.

Martinottiella spp.: includes *M. perparva* and *M. communis*.

Melonis spp.: represented by *M. padanum*, *M. soldanii*, and *M. cf. pompilioides*.

Nodosaria spp.: includes *N. longiscata* and *N. pentecostata* in Hole 975B, and *N. radicula* and *N. pentecostata* in Hole 974B.

Nonion gr.: groups the genera *Nonion* and *Nonionella* in both holes.

Oolina spp.: groups *O. heteromorpha*, *O. hexagona*, *O. intercalata*, and *O. squammosa*.

Ortomorphina spp.: comprises rare specimens of *O. havanensis* and *O. tenuicostata* in Hole 975B; *O. jedlitskai*, being more common, is plotted separately.

Pleurostomella spp.: includes an unnamed species, *P. alternans*, and *P. brevis*.

Pullenia spp.: comprises *P. bulloides*, *P. quinqueloba*, *P. quadriloba*, and *P. salisbury*.

Sigmoilopsis spp.: includes *S. schlumbergeri* and *S. celata*.

Spiroplectammina spp.: includes *S. carinata*, *S. deperdita*, and *S. depressa*.

Stilostomella spp.: represented in Hole 975B by *S. adolphina*, *S. annulifera*, *S. antillea*, *S. consobrina emaciata*, *S. fistula*, *S. modesta*, *S. monilis*, *S. pyrula* and some unidentified specimens; in Hole 974B this genus is represented by *S. consobrina*, *S. modesta*, and *S. monilis*.

Uvigerina spp.: in Hole 975B, groups *U. bononiensis*, *U. cf. hispida*, *U. cylindrica*, *U. rutila* and some unidentified specimens; in Hole 974B, only *U. bononiensis* and *U. proboscidea* are included.